Transactions of the Materials Research Society of Japan 30[2] 499-502 (2005)

Bismuth Substitution Effect on the Structure and Thermoelectric Properties of $[Ca_2CoO_3]_pCoO_2$

Yuzuru Miyazaki[1,4], Yousuke Suzuki[1], Mitsuko Onoda[2], Yoshinobu Ishii[3], Yukio Morii[3] and Tsuyoshi Kajitani[1,4]

1 Department of Applied Physics, Graduate School of Engineering, Tohoku University, Aramaki Aoba 6-6-05, Aoba-ku, Sendai, 980-8579 Japan, Fax: 81-22-217-7970, e-mail: miya@crystal.apph.tohoku.ac.jp

2 Advanced Materials Laboratory, National Institute for Materials Science, Namiki 1-1, Tsukuba, Ibaraki, 305-0044 Japan

3 Advanced Science Research Center, Japan Atomic Energy Research Institute, Shirakata Shirane 2-4, Tokai, Ibaraki, 319-1195 Japan

4 Core Research for Evolutional Science and Technology, Japan Science and Technology Agency, Nihonbashi 3-4-15, Chuo-ku, Tokyo, 103-0027 Japan

We have prepared Bi-substituted samples of the misfit-layered cobalt oxide $[Ca_2CoO_3]_{0.62}CoO_2$ and determined their crystal structure by a (3+1)-dimensional superspace group approach. The Bi atom substitute not only for Ca but also for Co in the rock salt-type subsystem, to form a solid solution $[(Ca_{1-x}Bi_x)_2(Co_{1-y}Bi_y)O_3]_{0.62}CoO_2$. Structural parameters have been refined assuming the superspace group of $C2/m(1p0)s0$ from powder neutron diffraction data. By the Bi substitution, the modulation of Co-O distances in the $[Ca_2CoO_3]$ subsystem markedly decreased relative to the Bi-free counterpart, whereas such a modulation amplitude in the $[CoO_2]$ subsystem slightly increased. The observed increase in the Seebeck coefficient and electrical resistivity of the Bi-substituted phase can be explained in terms of the decrease in hole concentration in the CoO_2 sheets.

Key words: thermoelectric compound, misfit layer, superspace group, substitution, Rietveld analysis

1. INTRODUCTION

Since the discovery of large Seebeck coefficient in $[Ca_2CoO_3]_{0.62}CoO_2$ (known as $Ca_3Co_4O_9$) [1-3], misfit-layered cobalt oxides have attracted much attention as candidate thermoelectric (TE) materials. The crystal structure of the cobaltite consists of an alternate stack of a distorted three-layered rock salt (RS)-type Ca_2CoO_3 block layer (BL) and a CdI_2-type CoO_2 conducting sheet parallel to the c-axis (Fig. 1) [2,4]. Owing to the size difference between the RS-type BL and the CoO_2 sheet, the compound has an incommensurate periodicity parallel to the b-axis, $p = b_{CoO2}/b_{RS} \sim 0.62$. Such an anisotropic structure is thought to be preferable to realize large Seebeck coefficient S and low thermal conductivity κ simultaneously, necessary for good TE compounds. For the practical use, an appreciable reduction of electric resistivity must be achieved because the room temperature resistivity ($\rho \sim 150$ μΩm) is about one order of magnitude larger than required. Much efforts have been devoted to reduce ρ while maintaining large S and low κ, through the partial substitution for the Ca atoms in the RS-type BL. Li *et al* [5]. prepared Bi-doped samples and reported a marked increase in TE performance. Funahashi *et al* [6]. succeeded in preparing single-crystalline samples with ZT ($= S^2T/\rho\kappa$) > 1 by partial substitution of Bi and Sr for Ca. However, the role of Bi was not clarified in these reports. We have determined the Bi-substitution in detail and discovered that the Bi atom simultaneously substitute for the Ca and Co sites in the RS-type subsystem. In this report, we present the preparation of the Bi-doped $[Ca_2CoO_3]_{0.62}CoO_2$ solid solution, structure analysis and TE properties of these samples. A small amount of Bi-substitution causes a large change in the modulation of CoO_2 conducting sheet and RS-type BL.

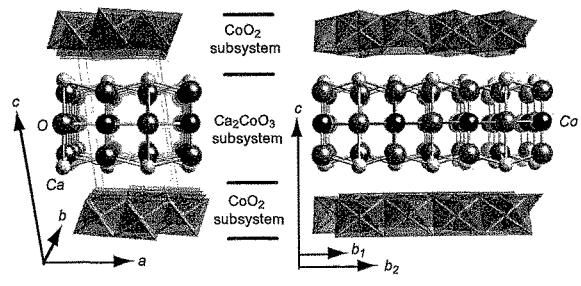

Fig. 1 Fundamental crystal structure of $[Ca_2CoO_3]_{0.62}CoO_2$.

2. EXPERIMENTAL

Polycrystalline samples were prepared by the standard solid-state reaction method. Appropriate amounts of $CaCO_3$ (99.9%), Bi_2O_3 (99.99%) and Co_3O_4 (99.995%) powders were mixed with an agate mortar

and pressed into pellets. The pellets were heated at 900 °C for 20 h in air and then furnace cooled to room temperature, ground and pelletized again. This process was repeated three times in order to obtain well-crystallized homogeneous samples. The solubility limit of Bi was determined on the basis of the structural work using an X-ray diffractometer (Rigaku RAD-X) equipped with a curved graphite monochromator. Neutron powder diffraction (ND) data were collected at 293 K using High Resolution Powder Diffractometer (HRPD) installed at JRR-3M reactor in Japan Atomic Energy Research Institute (JAERI). The XRD and ND data were analyzed using a Rietveld refinement program, PREMOS 91 [7], designed for modulated structure analyses.

The electrical resistivity was measured by the standard dc four-probe method. The thermoelectric power was determined by the conventional method. Both the measurements were performed from 300 K to 4 K.

3. RESULTS AND DISCUSSION

3.1 Preparation of the Bi-doped samples

We first attempted to substitute Bi for Ca, assuming the formula as $[(Ca_{1-x}Bi_x)_2CoO_3]_{0.62}CoO_2$. For this case, the solubility limit of Bi was quite small and the second phases appeared at $x > 0.02$. Then, we tried another substitution assuming that the Bi atom substitute only for the Co atom in the RS-type BL but no solid solution was formed. Unexpectedly, the single-phase region was found when we substituted Bi for the Ca and Co sites in the RS-type subsystem simultaneously. Figure 2 summarizes the determined single-phase region (closed circles) of the $[(Ca_{1-x}Bi_x)_2\ (Co_{1-y}Bi_y)O_3]_{0.62}CoO_2$ solid solution. The single-phase region lies in between the two lines denoted as the #1 and #2 series. In the #1 series, the Bi content changes with $x:y$ = 1:1, while that of the #2 series changes with $x:y$ = 2:1. The solubility limit of Bi is approximately $x = 0.06$ and $y = 0.06$ for #1 series and $x = 0.10$ and $y = 0.05$ for #2 series. Above these limits, the four-layered cobaltite $[Bi_2Ca_2O_4]_pCoO_2$ was detected as a minor phase.

Next, we examined the lattice parameters of the solid solutions by means of the Rietveld analysis. Due to the difficulty in refining modulation components from XRD data alone, the positional modulation of atomic sites was not taken into account for the fundamental structure refinements. The non-doped sample has the lattice parameters of a = 0.48323(3) nm, b_{CoO2} = 0.28217(2) nm, b_{RS} = 0.4565(1) nm, c = 1.08428(7) nm and b = 98.14(1)°. Both the two series showed similar x-dependence on the lattice parameters. With increasing x, all the axis lengths increased gradually, and the c-axis length showed the most significant expansion among the axes. This increase in the c-axis length corresponds to an expansion (~ 0.008 nm) of the interlayer distance of the CoO_2 sheets, which might effect the modulation of the Co-O bonds described below. However, the b-axis ratio remained nearly constant around p ~ 0.62, over the entire range of the solid solution. As we observed similar tendency between the #1 and #2 series, we will hereafter treat only the results of the #2 series.

3.2 Structural difference between the Bi-free and Bi-substituted samples

To compare the structural difference, we further analyzed the modulated structure of the Bi-free and the most Bi-substituted sample, *i.e.*, $x = 0.10$ and $y = 0.05$, using the ND data. The variation of the atomic positional modulation can be understood by the plot against t', a complementary coordinate in the (3+1)-dimensional superspace [7]. The upper left panel of Fig. 3 shows the Co-O distances in the RS-type subsystem of Bi-free $[Ca_2CoO_3]_{0.62}CoO_2$ plotted against t'. The Co2-O distances are periodically altered at an interval of $t' = 0.6181$, ranging from 0.17 to 0.27 nm. A Co atom at z = 1/2 has six oxygen neighbors, with four equatorial O2 and two apical O3 atoms. Among these bonds, two apical bonds (3 and 5) are fairly shorter than the other four equatorial bonds, ranging from 0.16 nm to 0.205 nm. The mean value of these distances is 0.180 nm. The four equatorial bonds range between 0.205 and 0.27 nm with a mean distance of 0.240 nm At t'~ 0 or 0.62, the Co2 and its surrounding six O atoms form a distorted CoO_6 octahedron, with one short Co2-O3 (3) and one long

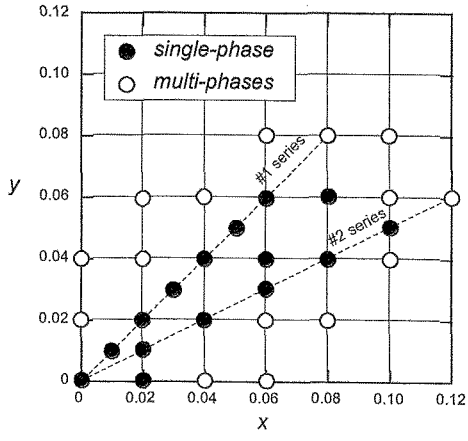

Fig. 2 Determined single-phase region for the Bi-substituted $[Ca_2CoO_3]_{0.62}CoO_2$ samples.

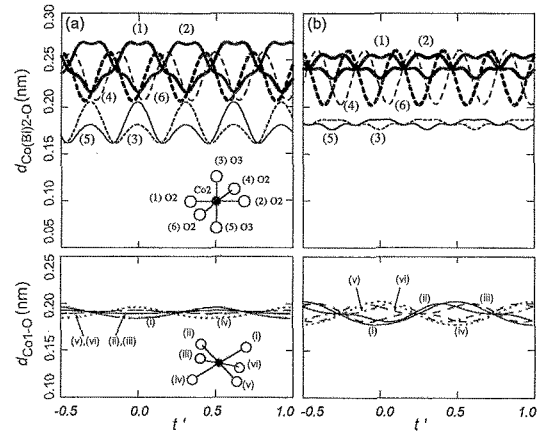

Fig. 3 The Co-O distances for the Bi-free and Bi-substituted $[Ca_2CoO_3]_{0.62}CoO_2$ samples.

Co2-O3 (5) apical bonds, almost equidistant three Co2-O2 (2, 4 and 6) bonds and another long Co2-O2 (1) bond.

When a small amount (5%) of Bi is substituted for Co2, the modulation amplitudes of the two apical Co(Bi)2-O3 bonds (3 and 5) are markedly decreased as illustrated in the upper right panel. However, the mean distance of the two bonds, 0.184 nm, does not change very much as that of the Bi-free one, 0.180 nm. A similar decrease in the modulation amplitudes is also observed for the two equatorial bonds (1 and 2), ranging from 0.225 to 0.25 nm, while the other two equatorial bonds along the incommensurate direction *b* (4 and 6), appear to show little change.

With regard to the [CoO_2] subsystem, the Co1-O1 bond length shows a periodical alteration with the periodicity equal to $\Delta t' = 1.0$. In contrast to the Co(Bi)2-O bonds, the six Co1-O1 bonds illustrated in the lower panels show an opposite substitution effect. The Co1-O1 bonds of the Bi-free phase (lower left panel) show small modulation amplitudes from 0.18 to 0.195 nm, relative to the Bi-substituted phase of 0.175 to 0.20 nm. Although, the mean distances of the Co1-O1 bonds of the two phases are almost equal, 0.191 nm, a large fluctuation in the bond lengths would be unfavorable for the electrical conduction. Of course, the electrical resistivity depends primarily on the hole concentration in the CoO_2 sheets.

3.3 Thermoelectric properties

Figure 4(a) shows the temperature dependence of the electrical resistivity $\rho(T)$ of the #2 series samples. The Bi-free sample exhibits ρ = 180 μΩm at 300 K and it shows metallic $\rho(T)$ behavior down to around T_{min} = 50 K. With further decrease in T, the sample turns to be insulating due to the occurrence of the spin-density-wave (SDW) transition. A small amount of Bi-substitution decreases ρ but further substitution decrease electric conductivity. The sample with x = 0.10 has ρ = 240 μΩm at 300 K and exhibits semiconducting behavior below 300 K.

Figure 4 (b) shows the temperature-dependent Seebeck coefficient $S(T)$ of the #2 series samples. All the samples show positive S values below 300 K. The Bi-free sample exhibits S = 140 μVK^{-1} at 300 K. With increasing Bi content, the absolute values of S gradually increase and it reaches S = 170 μVK^{-1} at 300 K for the sample with x = 0.10.

From the data of S and ρ, we can evaluate the TE power factor, S^2/ρ as a function of T. Fig. 5 represents the temperature dependence of S^2/ρ of #2 series samples. The Bi-free sample exhibits the power factor, ~100 μW/K^{2}m at room temperature. With decreasing T, the sample shows a broad maximum at around 150-200 K. With further decrease in T, the S^2/ρ value decreases steaply. When a small amount of Bi (x = 0.02) is incorporated, the S^2/ρ value increases more than 20 % and S^2/ρ shows as large as 160 μW/K^{2}m down to 150 K. Further increase in Bi deteriorates the power factor to a comparable value to that of the Bi-free sample, 110 μW/K^{2}m at 300 K.

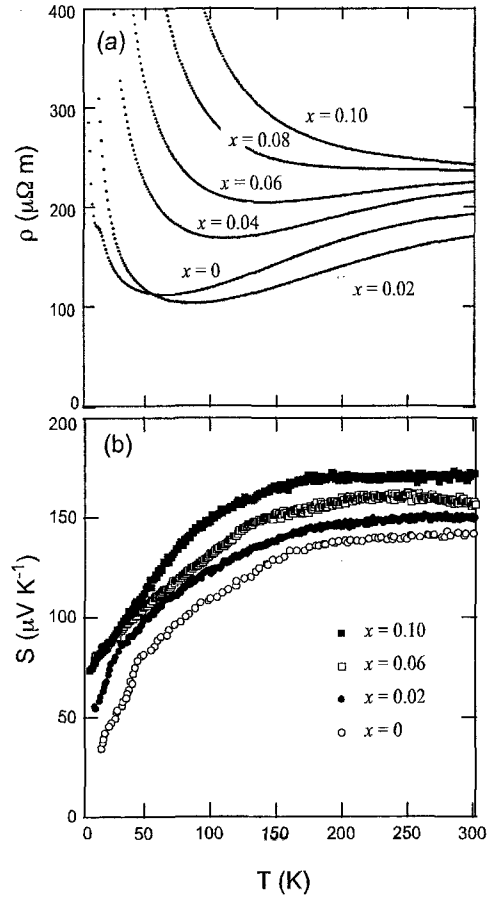

Fig. 4 Temperature dependence of the electrical resistivity ρ (a) and Seebeck coefficient S (b) of Bi-substituted $[Ca_2CoO_3]_{0.62}CoO_2$.

4. CONCLUDING REMARKS

It can be concluded that Bi plays different roles in the Ca and Co2 (RS) sites of the present $[Ca_2CoO_3]_{0.62}CoO_2$ system. When the Co2 site is the case, a small amount

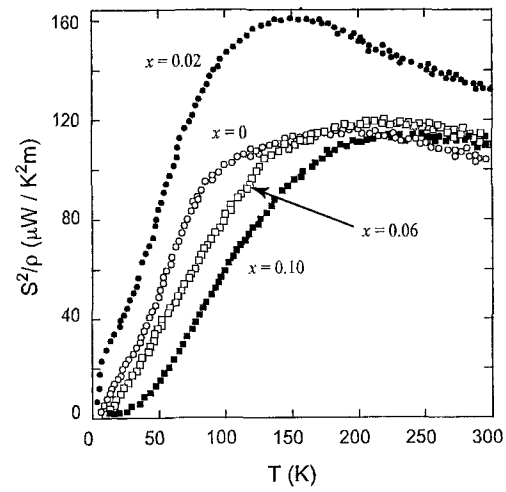

Fig. 5 Temperature dependence of the thermoelectric power factor S^2/ρ of Bi-substituted $[Ca_2CoO_3]_{0.62}CoO_2$.

(5%) of Bi markedly suppresses the modulation of the Co(Bi)2-O bonds. Moreover, such a substitution would dilute the spin correlation of Co^{4+} (S = 1/2) in the RS-type BL. The Ca^{2+} site can be partly substituted by Bi^{3+} up to ~10%. Accordingly, the Bi substitution mainly increases the valence state of the Ca(Bi) site without changing the valence of the Co(Bi)2 site. Since the RS-type BL can be regarded as a charge reservoir to introduce carriers into the CoO_2 sheet, such an increase in oxidation number decreases the hole concentration of the CoO_2 sheet. The modulation of the Co1-O bonds, enhanced by the Bi substitution, may also affect some transport properties. At high temperatures, the present Bi-substituted phase has been found to show a semiconducting $\rho(T)$ behavior while $S(T)$ tends to increase with T above room temperature. Then, the Bi-substituted phase would be advantageous for practical applications at high temperatures as reported by Li *et al* [5]. and Funahashi *et al* [6]. To maximize the TE properties at high temperatures, we are currently optimizing the concentration of Bi and other elements.

References

[1] S. Li, R. Funahashi, I. Matsubara, K. Ueno and H. Yamada, *J. Mater. Chem.* **9**, 1659-60 (1999).
[2] A. C. Masset, C. Michel, A. Maignan, M. Hervieu, O. Toulemomde, F. Atuder, B. Raveau and J. Hejtmanek, *Phys. Rev. B* **62**, 166-75 (2000).
[3] Y. Miyazaki, K. Kudo, M. Akoshima, Y. Ono, Y. Koike and T. Kajitani, *Jpn. J. Appl. Phys.* **39**, L531-33 (2000).
[4] Y. Miyazaki, M. Onoda, T. Oku, M. Kikuchi, Y. Ishii, Y. Ono, Y. Morii and T. Kajitani, *J. Phys. Soc. Jpn.* **71**, 491-97 (2002).
[5] S. Li, R. Funahashi, I. Matsubara, K. Ueno, S. Sodeoka and H. Yamada, *Chem. Mater.* **12**, 2424-27 (2000).
[6] R. Funahashi, I. Matsubara, H. Ikuta, T. Takeuchi, U. Mizutani and S. Sodeoka, *Jpn. J. Appl. Phys.* **39**, L1127-29 (2000).
[7] A. Yamamoto, *Acta Cryst.* **A 49**, 831-46 (1993).

(Received December 23, 2004; Accepted February 15, 2005)